Rapid convergence of time-averaged frequency in phase synchronized systems

Jörn Davidsen,[1,2,*] István Z. Kiss,[3] John L. Hudson,[3] Raymond Kapral[2,†]
[1]*Max-Planck-Institut für Physik komplexer Systeme, Nöthnitzer Strasse 38, 01187 Dresden, Germany*
[2]*Chemical Physics Theory Group, Department of Chemistry, University of Toronto, Toronto, Ontario, Canada M5S 3H6*
[3]*Department of Chemical Engineering, 102 Engineers' Way, University of Virginia, Charlottesville, Virginia 22904-4741, USA*
(Received 22 April 2003; published 26 August 2003)

Numerical and experimental evidences are presented to show that many phase synchronized systems of nonidentical chaotic oscillators, where the chaotic state is reached through a period-doubling cascade, show rapid convergence of the time-averaged frequency. The speed of convergence toward the natural frequency scales as the inverse of the measurement period. The results also suggest an explanation for why such chaotic oscillators can be phase synchronized.

DOI: 10.1103/PhysRevE.68.026217 PACS number(s): 05.45.Xt, 82.40.Np, 89.75.Da

I. INTRODUCTION

The rich collective behavior, including mutual entrainment and self-synchronization, in systems of coupled oscillators has been considered by several investigators in the past few years (see, for example, Refs. [1–3], and references therein). Recently, a considerable amount of research has been devoted to the study of coupled *chaotic* oscillators and, in particular, to the phenomenon of phase synchronization. Provided that the phase can be defined [4,5], two coupled nonidentical chaotic oscillators are said to be phase synchronized if their frequencies are locked but amplitudes are not [1,6]. This appears to be a general phenomenon and it has been observed in systems as diverse as electrically coupled neurons [7,8], biomedical systems [9], chemical systems [10], and spatially extended ecological systems [11]. Moreover, the potential role of phase synchronization in brain functions has been explored [12,13].

The most common theoretical approach to phase synchronization of chaotic oscillators is based on an analogy with the evolution of the phase of a periodic oscillator in the presence of external noise [1]. This approach leads to the conclusion that the dynamics of the phase is generally diffusive and the phase performs a random walk. However, the effective ''noise'' in such a description cannot be considered as a Gaussian δ-correlated noise in all circumstances. In this paper, we show that the effective noise exhibits strong temporal correlations for a general class of chaotic attractors. In particular, we present evidence from simulations and experiments that many phase synchronized systems of chaotic oscillators, where the chaotic state is reached through a period-doubling cascade, show a rapid convergence of the time-averaged frequency. The speed of convergence toward the natural frequency scales as the inverse of the measurement period. This implies that short measurement times may suffice for reliable determination of frequencies in those systems.

The outline of the paper is as follows. Section II presents a sketch of the theoretical background of phase dynamics in chaotic systems and the expected scaling of the time-averaged frequency with the observation time. The results of numerical simulations of globally coupled arrays of Rössler oscillators are presented in Sec. III where features of the chaotic attractor leading to rapid convergence of the time-averaged frequency are identified. Section IV contains a description and analysis of experimental results on a globally coupled array of electrochemical oscillators where rapid frequency convergence is observed.

II. THEORETICAL BACKGROUND

An appropriate definition of the phase for chaotic self-sustained oscillators can be obtained from the Poincaré map of the flow. Such a map can be constructed if a surface of section in the phase space of the autonomous continuous-time chaotic system exists which is crossed transversally by all trajectories of the chaotic attractor. Then, for each piece of a trajectory between two crossings of this surface, we define the phase as a linear function of time:

$$\phi(t) = 2\pi \frac{t - t_n}{t_{n+1} - t_n} + 2\pi n, \tag{1}$$

for $t_n \leqslant t < t_{n+1}$. Here, t_n is the time of the nth crossing of the surface of section. The definition is ambiguous because it depends on the choice of the Poincaré surface. Yet, any choice of a phase variable for chaotic oscillators investigated in this paper leads to the same macroscopic behavior [5].

With this phase definition, the phase dynamics can be described by

$$A_{n+1} = \mathcal{M}(A_n), \tag{2}$$

$$d\phi/dt = \omega(A_n) \equiv \omega_0 + \eta(A_n), \tag{3}$$

where the amplitude A_n is the set of coordinates of the phase point on the Poincaré surface at the nth intersection and $\mathcal{M}$ defines the Poincaré map that takes A_n to A_{n+1}. The ''instantaneous'' frequency $\omega(A_n) = 2\pi/T_n$ is determined by the Poincaré return time $T_n = t_{n+1} - t_n$ and depends, in general, on the amplitude. Assuming chaotic behavior of the amplitudes, we can consider the term $\omega(A_n)$ to be the sum of the average (natural) frequency ω_0 and some effective ''noise'' $\eta(A_n)$ with zero mean, although this stochastic term has a purely deterministic origin [1]. Thus, Eq. (3) has the solution

*Electronic address: davidsen@mpipks-dresden.mpg.de
†Electronic address: rkapral@chem.utoronto.ca

$$\phi(t) = \phi_0 + \omega_0 t + \int_0^t \eta(\tau) d\tau. \tag{4}$$

The variance of the integral $\int_0^t \eta(\tau) d\tau$ is given by

$$\left\langle \left(\int_0^t \eta(\tau) d\tau \right)^2 \right\rangle = 2 \int_0^t d\tau' (t-\tau') K(\tau')$$

$$\approx 2t \int_0^\infty d\tau' K(\tau') \equiv 2tD_\eta. \tag{5}$$

Here, $K(\tau') = \langle \eta(\tau)\eta(\tau+\tau') \rangle$ and the average $\langle \cdots \rangle$ is taken over the invariant measure of the chaotic attractor. The approximate equality holds provided that $\eta(\tau)$ has a finite correlation time t_c such that $K(\tau') \approx 0$ for $\tau' > t_c$ and one considers times $t \gg t_c$. This shows that the dynamics of the phase is diffusive and the phase performs a random walk as long as t_c is finite and $D_\eta \neq 0$. However, as pointed out by Pikovsky and co-workers [1], the dynamics of the phase generally differs from stochastic Brownian motion because the effective ''noise'' cannot be considered as a Gaussian white noise process. This was recently confirmed for a system of locally coupled Rössler oscillators where temporal correlations were shown to exist [14]. These correlations determine the speed of convergence of the time average $\overline{\omega}(T) = T^{-1}[\phi(T) - \phi(0)]$ toward ω_0. The speed of convergence—as measured by the standard deviation of the ensemble distribution of $\overline{\omega}(T)$—scales as $1/T$. This is in contrast to what one would expect if η was a white noise process where one obtains $1/\sqrt{T}$ scaling since $\overline{\omega}(T) - \omega_0 = 1/T \int_0^T dt\, \eta(t)$ and the standard deviation of $\int_0^T dt\, \eta(t)$ scales with $\sqrt{T}$. Here, we provide further numerical and experimental evidence that such a scaling generally occurs for oscillators where the chaotic state is reached through a period-doubling cascade. In particular, the type of coupling between the chaotic oscillators seems to be irrelevant. Moreover, we show that the temporal correlations induce an alternating behavior of $K(\tau')$. This leads to an extremely small value of D_η for these systems and suggests that they can generally be phase synchronized.

III. GLOBALLY COUPLED RÖSSLER OSCILLATORS

We consider an $L \times L$ array of *globally* coupled, nonidentical chaotic Rössler oscillators:

$$\frac{\partial \mathbf{x}(\mathbf{r},t)}{\partial t} = \mathbf{R}(\mathbf{x}(\mathbf{r},t)) + K/L^2 \sum_{\hat{\mathbf{r}} \in \mathcal{N}} [\mathbf{x}(\hat{\mathbf{r}},t) - \mathbf{x}(\mathbf{r},t)], \tag{6}$$

where $R_1 = -\omega(\mathbf{r})x_2 - x_3$, $R_2 = \omega(\mathbf{r})x_1 + 0.2x_2$, $R_3 = x_1 x_3 - 5.9x_3 + 0.2$. The sites of the lattice are labeled by $\mathbf{r}$, K is the coupling constant, and $\mathcal{N}$ is the set of all sites on the lattice. We take $L = 64$ and choose the $\omega(\mathbf{r})$'s randomly from a uniform distribution in the interval $[0.99, 1.01]$. This ensures that all oscillators are chaotic. We find that the speed of convergence of $\overline{\omega}(T)$ toward ω_0 in the phase synchronized state scales as $1/T$ (see Fig. 1). This is also true for higher $\omega(\mathbf{r})$ dispersion.

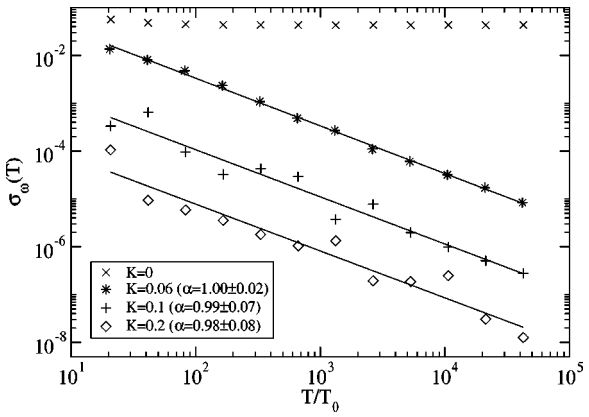

FIG. 1. Standard deviation $\sigma_{\overline{\omega}}(T)$ of the $\overline{\omega}(T)$ distribution in the phase synchronized state describing the speed of convergence toward ω_0. The datapoints for $K = 0.2$ are shifted down by one decade for clarity. The Poincaré surface was chosen as the surface spanned by the negative x_1 axis and the x_3 axis. The solid lines are best fits to the respective data and decay as $1/T^\alpha$. Note that $T_0 = 2\pi/\omega_0$ depends slightly on K.

The $1/T$ scaling observed in the globally coupled Rössler system follows from the fact that the local chaotic attractors, although one banded in the phase synchronized state (see Fig. 2), have internal structure.

In the absence of coupling ($K = 0$), the local nonidentical Rössler oscillators display a variety of banded chaotic attractors because of period-doubling cascades and period-3 windows in their vicinity. In the phase synchronized state for $K = 0.06$, the local chaotic attractors are very similar to one another and have an internal structure similar to that of a merged two-banded attractor. Although this structure is not obvious in the left panel of Fig. 2, it can be seen clearly in the local next amplitude maps (Fig. 3) and in the density distribution $\rho(l)$ (inset in Fig. 3). The intersection point of the map with the bisectrix defines four regions in the map such that the two bandedness of the attractor can be characterized by the percentage p of points in the upper left and lower right quarter planes. Indeed, only very few points ($1 - p = 3\%$)—typically those for small $A_{n,1}$'s which are in the lower left quarter plane of the amplitude map—stay in the same region of the bimodal density distribution, implying that the majority of the iterates map regions of high density

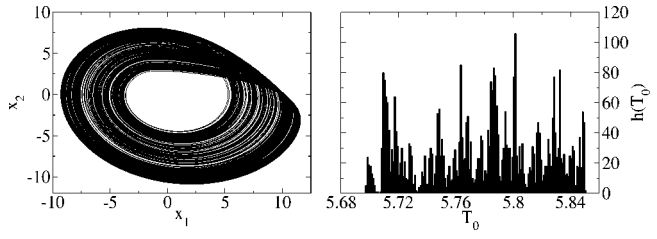

FIG. 2. Left panel: $x_1 - x_2$ projection of the local attractor at a single site of the lattice for $K = 0.06$ in the phase synchronized state. All local attractors look similar to the one shown here. Right panel: A typical $T_0 = 2\pi/\omega_0$ histogram $h(T_0)$ of the nonidentical chaotic oscillators for $K = 0$, i.e., the distribution of the natural periods. The exact shape of the distribution depends on the $\omega(\mathbf{r})$ realization.

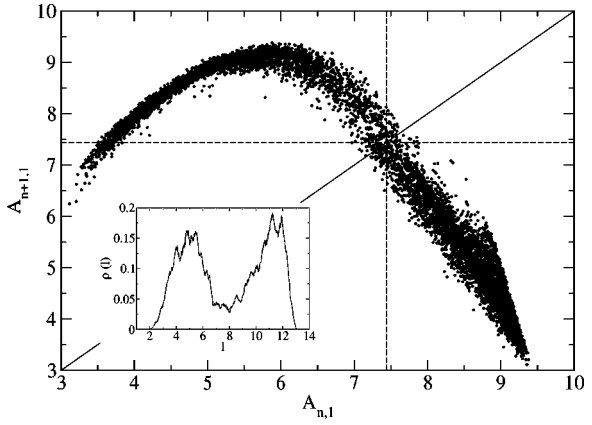

FIG. 3. Superposition of eight local next amplitude maps for $K=0.06$. The amplitude $A_{n,1}$ chosen here is the negative x_1 coordinate of A_n because the x_3 coordinate is almost constant and very close to zero. The dashed lines correspond to the intersection point of the bisectrix with the map. Inset: Density distribution $\rho(l)$ along the curve formed by the next amplitude maps.

on the left to regions of high density on the right and vice versa. This nearly two-banded character is also seen in the series of T_n's (see Fig. 4). An alternation of long and short return times can be observed with rare exceptions. This shows the close relation between topological characteristics (next amplitude map), and temporal evolution (T_n, T_{n+1} map) and suggests the following explanation for the observed scaling:

Assuming that each internal ''band'' of the attractor is associated with a distinct mean frequency ω_1 or ω_2 such that $\omega_0=2\omega_1\omega_2/(\omega_1+\omega_2)$, and the system alternates between bands, the ''random'' force in the evolution equation (3) for the phase of a single oscillator takes the form

$$\eta(t)=(-1)^{\kappa+1}\frac{\omega_\kappa(\omega_1-\omega_2)}{(\omega_1+\omega_2)}+\tilde{\eta}(t), \tag{7}$$

where $\kappa=1(2)$ when the system is on band 1(2). The noise term $\tilde{\eta}(t)$ accounts for deviations of the period within a band

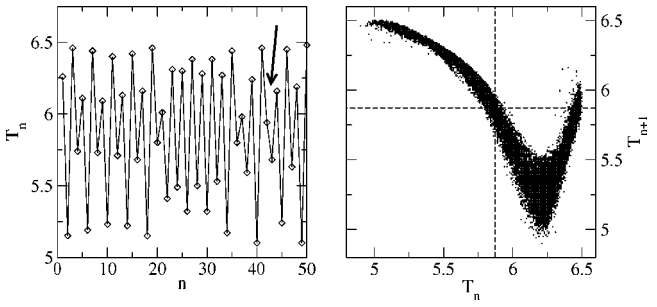

FIG. 4. Time series of T_n for $K=0.06$ (left panel) and the corresponding T_n, T_{n+1} map (right panel). The arrow highlights a deviation from the alternating behavior. These deviations occur with $1-p=2\%$ at this particular site of the lattice which is the percentage of points in the upper right and lower left quarter planes in the lower panel. Note that only a short segment of the T_n series is shown.

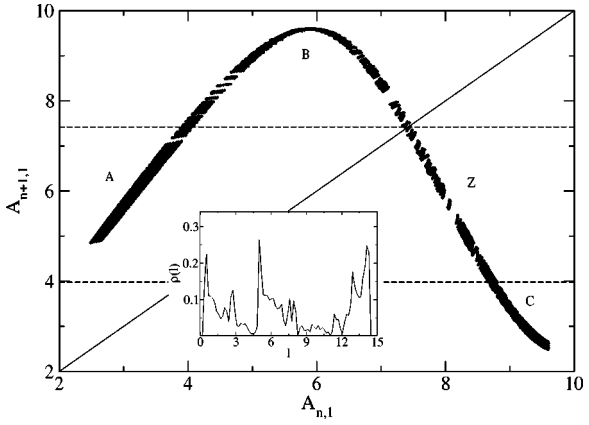

FIG. 5. Superposition of the next amplitude maps for $K=0.2$ at the same sites as in Fig. 3. Inset: Normalized point density along the curve formed by the next amplitude maps. Three regions of high density can be identified.

and deviations from the strict alternations between bands. If T is the time needed for n oscillations, it follows from Eq. (4) that

$$\overline{\omega}(T)-\omega_0 = \begin{cases} \int_0^T dt\,\dfrac{\tilde{\eta}(t)}{T}, & n \text{ even}, \\ (-1)^{\kappa+1}\dfrac{2\pi(\omega_1-\omega_2)}{(\omega_1+\omega_2)T}+\int_0^T dt\,\dfrac{\tilde{\eta}(t)}{T}, & n \text{ odd}, \end{cases} \tag{8}$$

where $\kappa=1(2)$ corresponds to band 1(2) appearing first in the series. The term $2\pi(\omega_i-\omega_j)/(\omega_1+\omega_2)T$ scales with $1/T$, while the term $\int_0^T dt\,\tilde{\eta}(t)/T$ scales with $1/\sqrt{T}$ provided that $\tilde{\eta}(t)$ is δ-correlated noise. Since the amplitude of the $1/\sqrt{T}$ term is very small, two scaling regimes can be identified for the maximal deviation from ω_0; a $1/T$ scaling on intermediate time scales which is dominated by the switching between the bands and a $1/\sqrt{T}$ scaling on long time scales. The intermediate time scale scaling behavior can indeed be observed for each oscillator; the envelope of $\overline{\omega}(T)-\omega_0$ decays as $1/T$. Note that the standard deviation of the ensemble distribution of $\overline{\omega}(T)$ decays as $1/\sqrt{T}$ for identical chaotic Rössler oscillators and $K=0$ — as expected from the law of large numbers. In the case of nonidentical oscillators, phase synchronization implies that the phases are synchronized such that $\sqrt{\langle(\overline{\omega}(T)-\omega_0)^2\rangle}$, where the average is taken over the ensemble, adopts the scaling of a single oscillator reproducing the observed scaling and explaining the results. This result does not depend on the type of coupling of the oscillators as confirmed by the numerical results presented here [15] and in Ref. [14]. This explanation is based exclusively on the fact that the series of the instantaneous frequencies alternates with the exception of rare events and that the system is phase synchronized.

The above argument easily generalizes to attractors with multiple internal bands which we observe in the phase synchronized state for higher coupling. Figure 5 shows that the

deviations from a three-banded structure are rather small for $K=0.2$. Three bands *A*, *B*, and *C* can be identified such that *A* is mapped to *B* and *C* to *A*. However, band *B* is mapped to *C* and *Z*, and *Z* back to *B* such that a pure three-banded structure does not exist. The invariant measure of the map in area *Z* is very low (approximately 10%).

The alternation of positive and negative values for $\eta(t)$ implies that $K(\tau')$ alternates as well. Hence, D_η is very small, i.e., a high degree of phase coherence persists. Our findings suggest that this should be generally expected for oscillators where the chaotic state is reached through a period-doubling cascade. Thus, these oscillators would be phase coherent suggesting that they can generically be phase synchronized.

The change in the structure of the local attractors as the coupling strength is changed is the analog of the bifurcation structure seen in homogeneous locally coupled Rössler oscillators where one finds period doubling different from the isolated Rössler oscillator [16].

IV. GLOBALLY COUPLED ELECTROCHEMICAL OSCILLATORS

We now study the convergence of the time-averaged frequency in an array of globally coupled electrochemical oscillators. A standard three electrode electrochemical cell consisting of a nickel working electrode array (64 1-mm diameter electrodes in an 8×8 geometry with 2 mm spacing), a $Hg/Hg_2SO_4/K_2SO_4$ reference electrode, and a Pt mesh counter electrode were used. The potentials of all of the electrodes in the array were held at the same value ($V=1.310$ V) with a potentiostat (EG&G Princeton Applied Research, model 273). Experiments were carried out in 4.5 M H_2SO_4 solution at a temperature of 11 °C. The working electrodes were embedded in epoxy and reaction takes place only at the ends. The currents of the electrodes were measured independently at a sampling rate of 100 Hz and thus the rate of reaction as a function of position and time was obtained.

The electrodes were connected to the potentiostat through 64 individual parallel resistors (R_p) and through one series collective resistor (R_s). We employed a method of altering the strength of global coupling while holding all other parameters constant. The total external resistance was held constant while the fraction dedicated to individual currents, as opposed to the total current, was varied. A total resistance can be defined as

$$R_{tot}=R_s+R_p/64. \tag{9}$$

In these experiments $R_{tot}=14.2\Omega$. The series resistor couples the electrodes globally. The parameter ε, the ratio of series to total resistance, is a measure of the global coupling

$$\varepsilon=\frac{R_s}{R_{tot}}. \tag{10}$$

For $\varepsilon=0$, the external resistance furnishes no additional global coupling; for $\varepsilon=1$, maximal external global coupling is achieved.

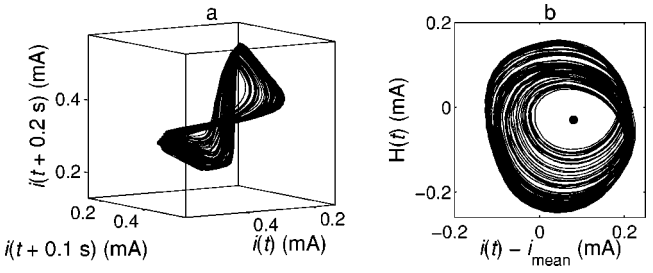

FIG. 6. Experiment. Chaotic dynamics of a single element at $\varepsilon=0.1$. (a) Reconstructed attractor using time delay coordinates. (b) Two-dimensional phase space reconstruction using the Hilbert transform. The solid circle represents the origin used for phase calculations.

The population of chaotic oscillators is characterized by certain amount of heterogeneity [10]. Without added coupling, there is a distribution of frequencies of the oscillators with a mean of 1.219 Hz and a standard deviation of 18 mHz. With weak added global coupling ($\varepsilon=0.1$), a nearly phase synchronized state occurs in which 63 of 64 oscillators have a frequency of 1.230 Hz, and that of the remaining element has a frequency of 1.237 Hz. The results are shown for this region of high phase synchrony.

Experimental Results

The chaotic attractor of a representative single element of the coupled system is shown in Fig. 6. The chaotic state is adjacent to a period-three window and a period doubling sequence. The reconstructed attractor [Fig. 6(a)] is low dimensional (correlation dimension 2.3 ± 0.1). To obtain the phase, the Hilbert transform approach is applied [1]. The two-dimensional embedding using Hilbert transform is shown in Fig. 6(b). As in the case of globally coupled Rössler oscillators, it is difficult to distinguish the banded character of the attractor.

The merged banded structure is more clearly seen in return maps obtained from the series of return times T_n. The series of the return time clearly shows an alternation of long and short oscillations [Fig. 7(a)]. The map constructed using T_n exhibits an approximately one-dimensional (1D) character [Fig. 7(b)].

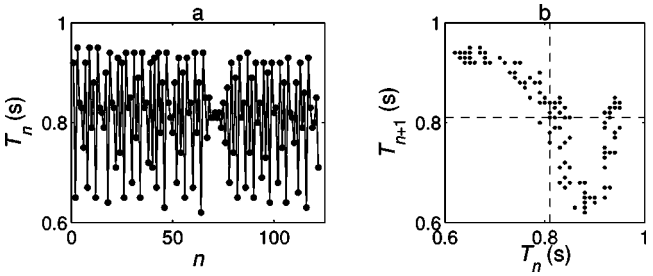

FIG. 7. Experiment. Time series and maps of discretized chaotic dynamics of a single element at $\varepsilon=0.1$. (a) Time series of return times T_n of the oscillations. (b) One-dimensional map using the return time. The dashed lines correspond to the average period of oscillations ($T_0=0.81$ s) which in this case is identical to the intersection of the map with the bisectrix.

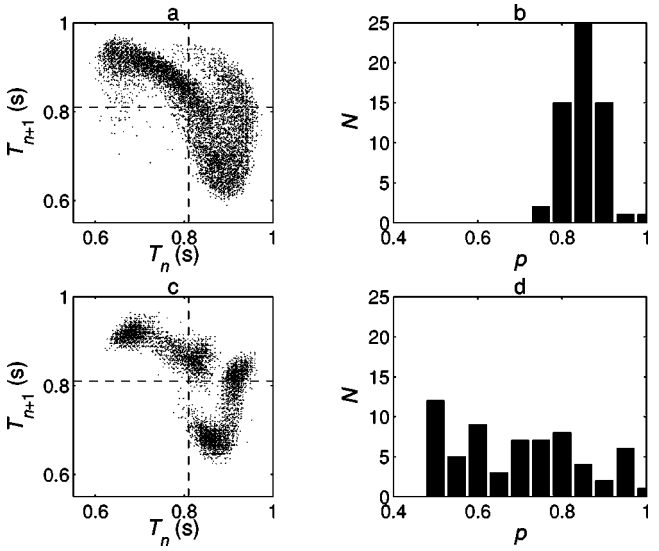

FIG. 8. Experiment. Characterization of the two-banded character of the population 64 oscillators. Top row: $\varepsilon=0.1$. Bottom row: $\varepsilon=0$. (a) Superimposed one-dimensional maps of the 64 sites. The dashed lines correspond to the average period of oscillations ($\overline{T}=0.81$ s); $\varepsilon=0.1$. (b) The distribution of probability p of two-banded oscillations; $\varepsilon=0.1$. (c) Superimposed one-dimensional maps of the 64 sites; $\varepsilon=0$. (d) The distribution of probability p of two-banded oscillations; $\varepsilon=0$.

The oscillators in the population are slightly different. Figure 8(a) shows a superposition of the 1D maps of all the oscillators. Clearly, the majority of the phase points lie in the upper left and lower right boxes indicating two-banded character. The probability of two-banded oscillations varies from one site to the other [Fig. 8(b)] with a mean of $p_{mean}=0.85$ and a standard deviation of 0.05. We note that the two-banded character of the uncoupled system of uncoupled oscillators [$\varepsilon=0$, $p_{mean}=0.7$, Figs. 8(c) and 8(d)] is smaller than that of the phase synchronized region. Therefore, during the transition to phase synchronization with increasing the coupling strength, the two bandedness observed in the time series of oscillations is more pronounced.

As expected from the numerical simulations and theoretical considerations, the strong correlations in the phase dynamics have pronounced effects on the speed of convergence of frequencies. Figure 9 shows that the standard deviation of frequencies is proportional to $1/T$ at $\varepsilon=0.1$. (The fluctuations around the fitted line are caused by slowing down and speeding up within a cycle.) Similar scaling results are obtained for other (larger) coupling strengths.

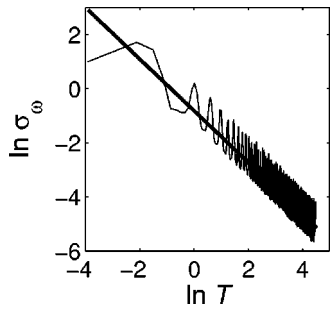

FIG. 9. Standard deviation of the experimental frequency distribution as a function of the applied time average (the thick line is a linear fit with slope -0.97) for $\varepsilon=0.1$.

V. CONCLUSION

For many systems of coupled oscillators, the chaotic state is reached through a period-doubling cascade. This implies that a Poincaré surface exists such that the next-amplitude map is similar to that in Fig. 3 or 5. As long as the correspondence between the next-amplitude map and the relation of subsequent return times holds, this should lead to a small value of D_η and, in particular, to a $1/T$ scaling in the phase synchronized state. The experimental results show that such a structure of the series of return times can exists even if no well-behaved next-amplitude map can be identified. Our findings further suggest that chaotic oscillators where the chaotic state is reached through a period-doubling cascade can generally be phase synchronized due to the small value of D_η, i.e., high degree of phase coherence. This is in accord with findings in Ref. [1] where different chaotic systems were analyzed with respect to their ability to be phase synchronized. There it was found that the Lorenz system (where the chaotic attractor is not reached through a period-doubling cascade) cannot be phase synchronized. In particular, the next-amplitude map has a very different structure, i.e., a logarithmic singularity.

Finally, in many biological and physical systems, only short time series are available. Our results show that the determination of frequencies in weakly coupled oscillatory systems may be obtainable from such short time series.

ACKNOWLEDGMENTS

This work (J.L.H. and I.Z.K.) was supported in part by the National Science Foundation (Grant No. CTS-0000483) and the Office of Naval Research (Grant No. N00014-01-1-0603). R.K. and J.D. were supported in part by a grant from the Natural Sciences and Engineering Research Council of Canada. We thank Yumei Zhai for help with the experiments.

[1] A.S. Pikovsky, M. Rosenblum, and J. Kurths, *Synchronization: A Universal Concept in Nonlinear Science* (Cambridge University Press, Cambridge, U.K., 2001).
[2] S.H. Strogatz, Physica D **143**, 1 (2000).
[3] Y. Kuramoto, *Chemical Oscillations, Waves, and Turbulence* (Springer-Verlag, Berlin, 1984).
[4] A.S. Pikovsky, M.G. Rosenblum, G.V. Osipov, and J. Kurths, Physica D **104**, 219 (1997).
[5] K. Josić and D.J. Mar, Phys. Rev. E **64**, 056234 (2001).
[6] M. Rosenblum, A.S. Pikovsky, and J. Kurths, Phys. Rev. Lett. **76**, 1804 (1996).
[7] R.C. Elson, A.I. Selverston, R. Huerta, N.F. Rulkov, M.I.

Rabinovich, and H.D.I. Abarbanel, Phys. Rev. Lett. **81**, 5692 (1998).
[8] V. Makarenko and R. Llinás, Proc. Natl. Acad. Sci. U.S.A. **95**, 15474 (1998).
[9] C. Schäfer, M.G. Rosenblum, J. Kurths, and H.H. Abel, Nature (London) **392**, 239 (1998).
[10] I.Z. Kiss, Y. Zhai, and J.L. Hudson, Phys. Rev. Lett. **88**, 238301 (2002); Ind. Eng. Chem. Res. **41**, 6363 (2002); I.Z. Kiss and J.L. Hudson, Phys. Chem. Chem. Phys. **4**, 2638 (2002).
[11] B. Blasius, A. Hupert, and L. Stone, Nature (London) **399**, 354 (1999).
[12] R. Fitzgerald, Phys. Today **52**(3), 17 (1999).
[13] P.A. Tass, T. Fieseler, J. Dammers, K. Dolan, P. Morosan, M. Majtanik, F. Boers, A. Muren, K. Zilles, and G.R. Fink, Phys. Rev. Lett. **90**, 088101 (2003).
[14] J. Davidsen and R. Kapral, Phys. Rev. E **66**, 055202(R) (2002).
[15] For local (next-neighbor) coupling, we obtain results qualitatively similar to those shown in Figs. 2, 3, and 4.
[16] A. Goryachev, H. Chaté, and R. Kapral, Int. J. Bifurcation Chaos Appl. Sci. Eng. **10**, 1537 (2000).